



Photoluminescence properties and synthesis of a PZT mesostructure obtained by the microwave-assisted hydrothermal method

G.F. Teixeira^{a,*}, M.A. Zaghete^a, G. Gasparotto^a, M.G.S. Costa^a, J.W.M. Espinosa^b, E. Longo^a, J.A. Varela^a

^a Laboratório Interdisciplinar de Eletroquímica e Cerâmica (LIEC), Instituto de Química, UNESP, CP 355, 14801-907 Araraquara, SP, Brazil

^b Universidade Federal de Goiás, Câmpus de Catalão, Engenharia de Produção, Avenida Dr. Lamartine Pinto de Avelar, 1120 CEP 75700-000, Brazil

ARTICLE INFO

Article history:

Received 14 December 2010

Received in revised form

13 September 2011

Accepted 14 September 2011

Available online 29 September 2011

Keywords:

PZT

Perovskite

Photoluminescence

Microwave hydrothermal synthesis

ABSTRACT

Micro-cube-shaped lead zirconate titanate was synthesized using the microwave-assisted hydrothermal method. Photoluminescence and field emission scanning electron microscopy were used for monitoring the formation of mesocrystals. Based on these results, a growth mechanism was then proposed which involved nanoparticle aggregation, nanoplate self-assembly on specific architecture and the final formation of mesoscopic micro-cube-shaped lead zirconate titanate.

© 2011 Elsevier B.V. All rights reserved.

1. Introduction

A lead zirconate titanate (PZT) semiconductor with band gap energy around 2.96–3.72 eV has been extensively studied due to its excellent ferroelectric, dielectric and piezoelectric properties; however, there have been very few research studies regarding its semiconducting behavior [1,2]. In particular, for decades, the PZT solid solution obtained by the oxide mixture and Pechini method has dominated the technological field responsible for the development of piezoelectric and ferroelectric materials [3,4]. An important problem in the fabrication of PZT ceramics by these techniques is the volatility of PbO at high temperatures, which leads to the fluctuation in the PZT composition [5]. Also, the ceramics synthesized at high temperatures often exhibit drawbacks such as lower chemical activity, higher impurity content and large particle sizes making them unsuitable for device applications. As an alternative to the use of micro-fabrication processing, the microwave hydrothermal (MAH) method has increasingly attracted attention in recent times from the viewpoint of its morphology and growth mechanism involving hierarchical structures [6,7].

Oriented aggregation is a non-classical crystal growth mechanism that involves the self-assembly of primary nanocrystals, crystallographic reorganization within the self-assemblies and its conversion into oriented aggregates which are new crystals [8,9].

The nanoparticle building units in a mesocrystal are all crystallographically perfect and are fused together to eliminate surface defects and thus decrease the total system energy [10]. To date, this complicated process has hampered the investigation of the transformation of a mesocrystal into a single crystal. On the other hand, as an interesting example of a non-classical crystallization product, a mesocrystal not only exhibits an abundance of bound nanocrystals, but also presents nearly identical crystallographic orientations among nanoparticle building units such as single crystals. Therefore, a mesocrystal is known to possess quite different physical characteristics such as interface effects as well as different optical properties [11]. Undoubtedly, these physical characteristics are closely related to the spherical structure of mesocrystals. The formation of a mesocrystal has been suggested as a necessary intermediate step to oriented aggregation which can lead to the production of anisotropic nanoparticles with high yields and size control [12–14]. Oriented aggregation also provides the potential to tune material properties by controlling defect concentrations (order–disorder), morphology and size as well as size distribution.

Optical properties such as photoluminescence (PL) depend on both structural and electronic properties, including the morphological and structural control of primary building blocks. PL depends highly on electronic excitations which thus make it a necessary complement to spectroscopy regarding lattice excitations to yield structural information of a different character from the information obtainable by diffraction-based techniques. The diffraction-based techniques identify long-range order defects while it is possible

* Corresponding author. Tel.: +55 16 3301 9712; fax: +55 16 3301 9707.
E-mail address: mina.guilher@gmail.com (G.F. Teixeira).

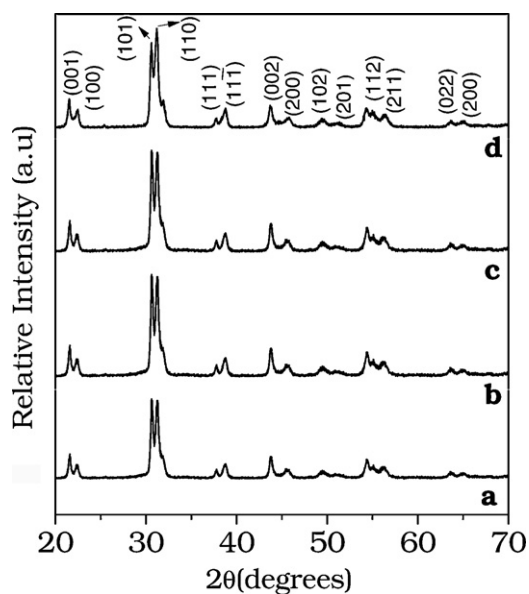


Fig. 1. XRD patterns of PZT powders obtained by microwave hydrothermal method for different time periods: (a) 2 h, (b) 6 h, (c) 8 h and (d) 12 h.

to obtain intermediate and short order defects information using PL. In this regard, PL spectroscopy can be said to be a sensitive, no-contact and non-destructive method suitable for the characterization of the extrinsic, native or intrinsic defects of materials, and the PL spectrum is known to be the result of a clear quantum effect [15,16].

The purpose of the present study is to investigate the conditions necessary to obtain PZT powders synthesized by the MAH method to characterize luminescence properties and to correlate them with a structural order–disorder degree of PZT-MAH crystalline samples.

2. Experimental procedures

The ratio of Zr/Ti = 52/48 corresponds to the composition of the desired PZT product which was synthesized using $\text{Pb}(\text{NO}_3)_2$ (Mevryinckrot, 99.7%), $\text{ZrOCl}_2 \cdot 8\text{H}_2\text{O}$ (Riedel-deHaen, 99.8%), TiO_2 (Vetec-Ltda 99.8%) and KOH (J. T. Baker 87.2%) as mineralizing agent. First, a suspension containing $\text{Pb}(\text{NO}_3)_2$ and $\text{ZrOCl}_2 \cdot 8\text{H}_2\text{O}$ was prepared. A suspension of TiO_2 and KOH solution (1.8 mol L^{-1}) was also added which resulted in a precursor with a concentration of 0.31 mol L^{-1} of PZT. The precursor was kept at room temperature under stirring for approximately 20 min. Then it was loaded into a 90 ml Teflon vessel occupying 30% of its volume which provided maximum pressure efficiency to the system. The vessel was then sealed and placed in the microwave furnace for the synthesis of PZT powder. The synthesis temperature was 180°C , and the varying times used were 2, 6, 8 and 12 h. The solid product was then washed with distilled water until a neutral pH was obtained and was dried afterwards at room temperature. A MAH digester (MARS-CEM, USA) was used for the synthesis.

The powders obtained were characterized by X-ray diffraction (XRD) using a Rigaku, model D/Max-2500/PC, Cu $\text{K}\alpha$ radiation in the 2θ range of 20° – 70° with $0.02^\circ/\text{min}$. Ultraviolet–visible absorption spectroscopy of crystalline PZT powders was performed using Cary 5G equipment (USA). Photoluminescence (PL) spectroscopies were carried out using a U1000 Jobin-Yvon double monochromator coupled to a cooled GaAs photomultiplier with a conventional photon counting system. The 488 nm excitation wavelength of an argon ion laser was used; its maximum output power was kept at 200 mW. The morphology and microstructure of the powder was visualized by field emission scanning electron microscopy (FE-SEM) using ZEISS SUPRA 35 microscope.

3. Results and discussion

The crystallinity of the PZT micro-cubes was confirmed using the XRD pattern (see Fig. 1). The synthesis at 180°C from 2 h onward enabled us to obtain crystalline PZT with all the peaks indexed as a PZT tetragonal phase with lattice parameters $a = 4.036 \text{ \AA}$ and $c = 4.146 \text{ \AA}$ which are in accord with the standard data from the Joint Committee on Powder Diffraction Standards (JCPDS) card no 33-784. No impurity phases were detected in the experimental range.

Fig. 2(a)–(d) obtained by field emission scanning electron microscopy (FE-SEM) shows general morphologies of the samples. The formation of the PZT mesostructure is characterized by bigger cubes which are previously formed and smaller cubes that

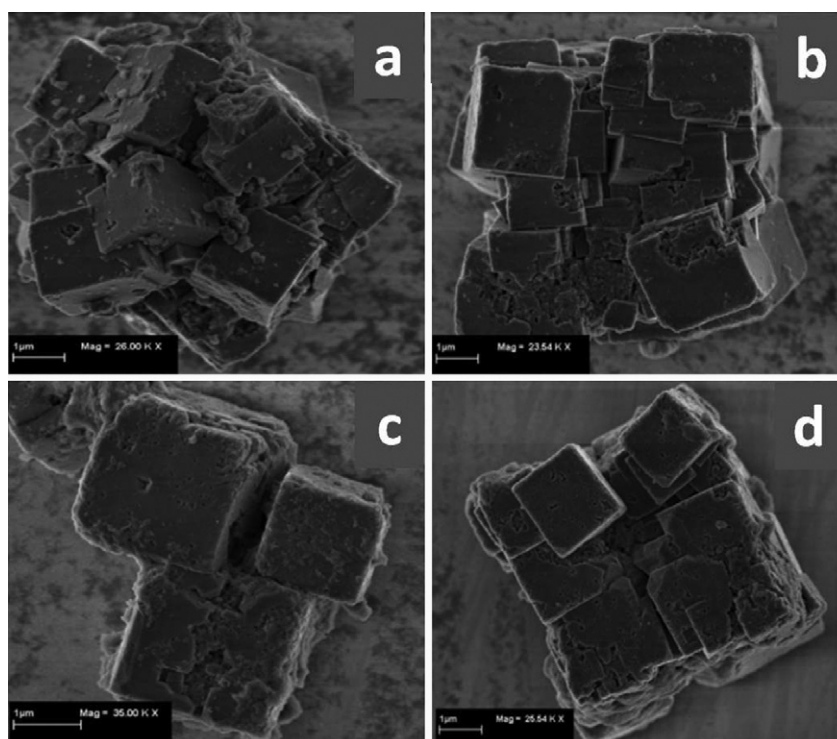


Fig. 2. FE-SEM images of PZT mesocrystals synthesized by MAH at different times: (a) 2 h, (b) 6 h, (c) 8 h and (d) 12 h.

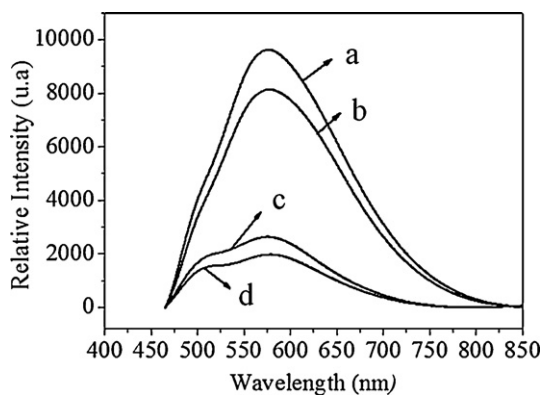


Fig. 3. Photoluminescence spectra at room temperature of PZT powders obtained by microwave hydrothermal method for different time periods: (a) 2 h, (b) 6 h, (c) 8 h and (d) 12 h.

originate from the bigger ones with a uniform shape and different sizes. The cubes that form the mesostructures have edges and surfaces that look corroded as can be clearly observed in all samples. Interestingly, the PZT architecture is composed of many well-aligned crystal nanoplates which exhibit a layered pattern. It can be observed that the nanoplates can self-assemble forming a cubic architecture along the longitudinal and horizontal axes in the absence of any specific additives or templates. The plates are attached to an integrated structure showing that the cubes originate from each other.

The PL spectroscopy is an effective way to investigate the electronic structure as well as the optical properties of semiconductor materials [17]. Important information such as surface defects, oxygen vacancies, surface states, photo-induced charge carrier separation and a recombination process in nano-size semiconductor materials can be obtained from PL spectroscopy.

PL emissions of PZT mesocrystals along the synthetic route are shown in Fig. 3. For the different times of synthesis investigated here, the photoluminescence intensity is found to be in the region of approximately 600 nm (corresponding to a green emission region), besides, the emission decreases with increasing synthesis time which is related to structural and/or surface defects generated

during the synthesis. According to Rout [18] the structural defects observed in these super cells can be attributed to oxygen vacancies and/or distortions which present three different charge states: (a) neutral (V_O^x) – captures two electrons, (b) single ionized (V_O^\bullet) – captures only one electron and (c) double ionized ($V_O^{\bullet\bullet}$) – it is unable to trap electrons. Double-charged oxygen vacancies ($V_O^{\bullet\bullet}$) are the most mobile charge carriers in a structure and assume an important role in the conduction mechanism. Oxygen vacancies are known as deep defects (responsible for emission in the violet and blue region) and distortions of clusters are known as shallow defects (responsible for emission in the green, yellow and red region). In this study, an increase in synthesis time tends to decrease surface defects or distortions resulting in lower emission of the photoluminescence intensity.

The PL curves in Fig. 4(a)–(d) show three components: blue (maximum below 2.43 eV), green (maximum below 2.21 eV) and yellow (maximum below 2.00 eV). The intermediary energy levels are strongly affected by time processing as a result of a more ordered structure of the PZT mesocrystals in the following sequences: 2, 6, 8 and 12 h of PZT synthesis time-periods.

In the first stages where the microcrystals are assembled to form mesocrystals, it is necessary to surmount energy barriers to form PZT nanoplates. The PL behavior during this self-assembly process can be assigned to surface defects generated in the joining of the different nanoplates. During the growth stages, mesocrystals do not have a stable structure and morphology. Due to structural defects, the PL intensities increase in the blue-green region and decrease in the yellow region. This interesting result confirms the density of defects in nanostructured PZT microcubes. Previous studies had shown that the PL emission was related to the oxygen vacancy in the crystal structure [19]. For the fact that PL emissions are very sensitive to structural disorder, they can provide necessary information concerning the disorder degree of the mesocrystal as can be deduced from the analysis of Figs. 2 and 3.

Long-range ordered powders present well-defined line absorption while short- and medium-range disordered powders exhibit a typical continuous smooth absorption which increases as a result of the states located inside the band gap. Using the Wood and Tauc method [20], the optical gap for powders synthesized for 2, 6, 8 and 12 h was obtained by the extrapolations of the linear curve

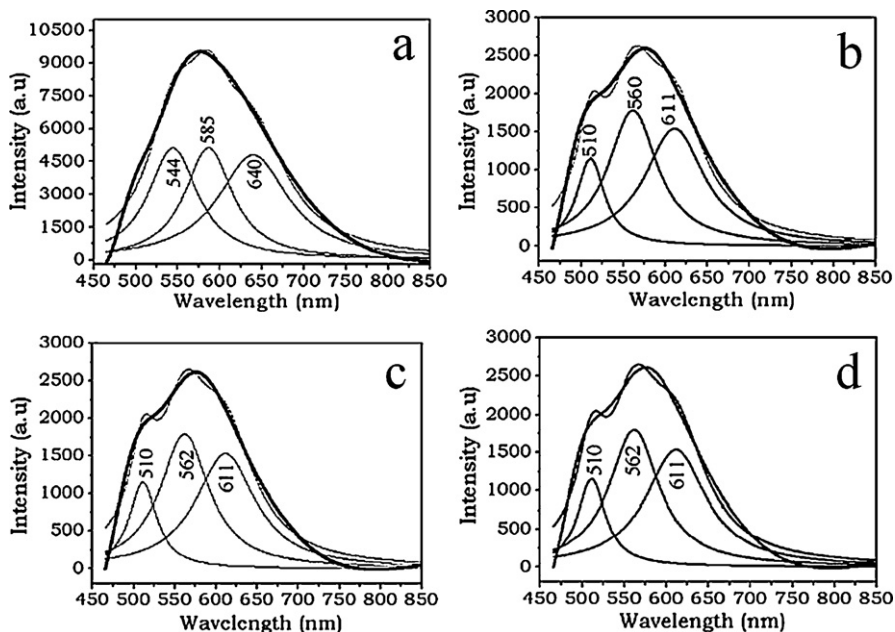


Fig. 4. Deconvolution of photoluminescence curves of PZT powders: (a) 2 h, (b) 6 h, (c) 8 h and (d) 12 h.

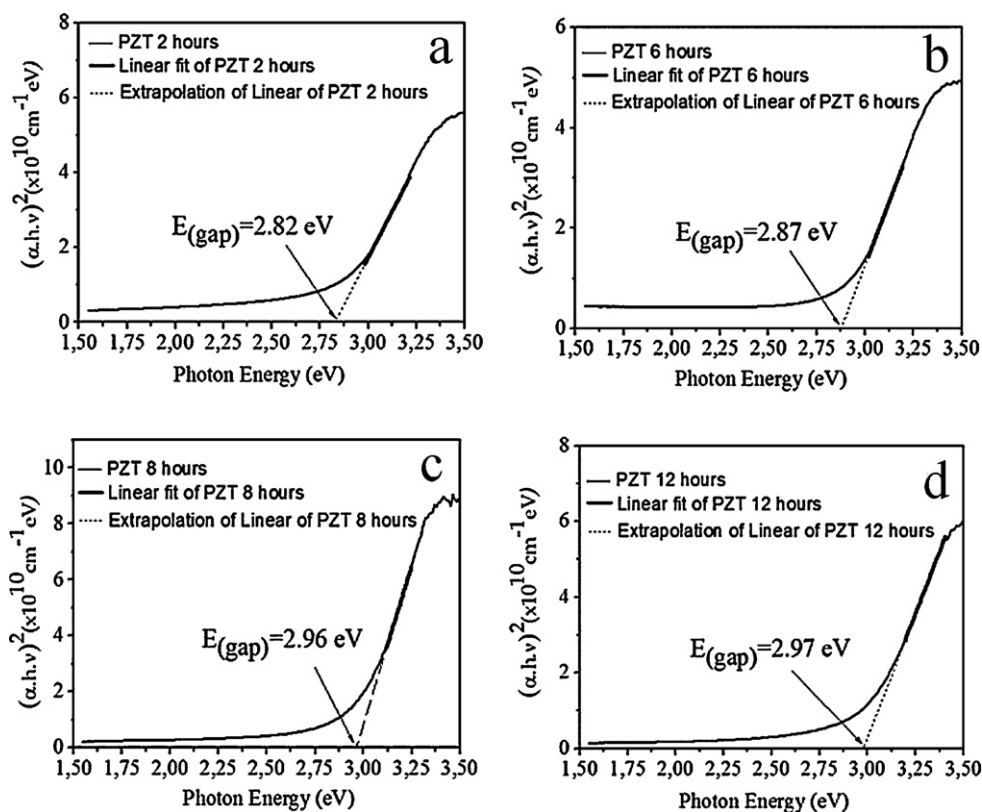


Fig. 5. UV-visible absorbance spectra of PZT powders obtained by MAH method for varying synthesis time periods: (a) 2 h, (b) 6 h, (c) 8 h and (d) 12 h.

regions of the spectral absorbance. The values obtained were 2.82, 2.87, 2.96 and 2.97 eV, respectively (see Fig. 5). Liu et al. on the other hand, obtained an optical gap value of 3.2 eV in the region [21] for the PZT ordered sample. These results indicate that the exponential optical absorption edge and the optical band gap energy are controlled by the degree of structural disorder in the mesocrystals.

4. Conclusion

In summary, this paper offers a detailed report of PL results and a systematic analysis of PZT powders obtained by the MAH method. XRD patterns provide evidence that it is possible to obtain PZT mesocrystals without a secondary phase from 2 h of synthesis onwards at 180 °C. The FE-SE micrographs show a PZT microcube with a uniform shape and different sizes. The increase in band gap of PZT powders is proportional to the increase in the synthesis time. Under 488 nm photoexcitation, the observed PL curves are composed of blue, green and yellow components, and the largest contribution of the emission is the green component (around 600 nm). An increase in the synthesis time was found to decrease surface defects which thus results in a decrease in the PL intensity. The results indicate that the use of photoluminescence is an effective technique that identifies the presence of defects in the PZT mesostructure. In addition, the PL emission of this material that is clearly observed shows that beyond ferroelectric applications that are well known in the literature, the PL is an interesting additional property for technological applications.

Acknowledgement

The authors would like to express their gratitude and indebtedness to UNESP-Chemistry Institute of Araraquara, Department of

Biochemistry and Chemical Technology, for offering the necessary structural and personnel working conditions for the development of this work.

References

- [1] G. Suchanek, D. Chvostová, J. Kousal, V. Železný, A. Lynnyk, L. Jastrabík, G. Gerlach, A. Dejnek, *Thin Solid Films* 519 (2011) 2885–2888.
- [2] G.F. Teixeira, G. Gasparotto, E.C. Paris, M.A. Zaghete, E. Longo, J.A. Varela, *J. Lumin.* 132 (2012) 46–50.
- [3] K. Vojisavljević, G. Branković, T. Srećković, A. Rečnik, Z. Branković, *J. Eur. Ceram. Soc.* 30 (2010) 485–488.
- [4] P. Jaita, A. Watcharapasorn, S. Jiansirisomboon, *Solid State Sci.* 12 (2010) 1608–1614.
- [5] V.A. Chaudhari, G.K. Bichile, *Physica B* 405 (2010) 534–539.
- [6] F.V. Motta, R.C. Lima, A.P.A. Marques, M.S. Li, E.R. Leite, J.A. Varela, E. Longo, *J. Alloys Compd.* 497 (2010) L25–L28.
- [7] A.Z. Simões, F. Moura, T.B. Onofre, M.A. Ramirez, J.A. Varela, E. Longo, *J. Alloys Compd.* 508 (2010) 620–624.
- [8] R.L. Penn, *J. Phys. Chem.* 108 (2004) 12707–12712.
- [9] R.L. Penn, J.F. Banfield, *Science* 281 (1998) 969–971.
- [10] T.X. Wang, H. Colfen, M. Antonietti, *J. Am. Chem. Soc.* 127 (2005) 3246–3247.
- [11] J. Fang, B. Ding, X. Song, Y. Ham, *Appl. Phys. Lett.* 92 (2008) 173120–173120.
- [12] M. Niederberger, H. Coelfen, *Phys. Chem. Chem. Phys.* 8 (2006) 3271–3287.
- [13] M.L. Moreira, E.C. Paris, G.S. Nascimento, V.M. Longo, J.R. Sambrano, V.R. Mastelaro, M.L.B. Bernardi, J. Andrés, J.A. Varela, E. Longo, *Acta Mater.* 57 (2009) 5174–5185.
- [14] A.E. Souza, R.A. Silva, G.T.A. Santos, S.R. Teixeira, S.G. Antonio, M.L. Moreira, D.P. Volanti, E. Longo, *Chem. Phys. Lett.* 514 (2011) 301–306.
- [15] W.H. Zhang, J.X. Zhang, *J. Lumin.* 131 (2011) 2307–2310.
- [16] F.V. Motta, A.P.A. Marques, J.W.M. Espinosa, P.S. Pizani, E. Longo, J.A. Varela, *Curr. Appl. Phys.* 10 (2010) 16–20.
- [17] V.M. Longo, M.S. Silva, A.T. Figueiredo, R.W.A. Franco, C. Vila, M. Cilense, J.A. Varela, E. Longo, J. Andrés, *Chem. Phys. Lett.* 4754 (2009) 96–100.
- [18] S.K. Rout, L.S. Cavalcante, J.C. Sczancoski, T. Badapanda, S. Panigrahi, M.S. Li, E. Longo, *Physica B* 404 (2009) 3341–3347.
- [19] E.R. Leite, F.M. Pontes, E.C. Paris, C.A. Paskocimas, E.J.H. Lee, E. Longo, P.S. Pizani, J.A. Varela, V. Mastelaro, *Adv. Mater. Opt. Electron.* 10 (2000) 235–240.
- [20] J. Tauc, D.L. Wod, *Phys. Rev. B* 5 (1972) 3144–3151.
- [21] Y. Liu, C.H. Xu, K. Nonaka, H. Tateyama, *Ferroelectrics* 264 (2001) 331–336.